Analyzing Lithology Generated Seismic Avo Anomaly In Deep Water Well In Indian Basin

NK Khatri*, PK Chaudhuary

IRS, ONGC, Chandkheda, Ahmedabad 380005

Abstract

Low impedance hydrocarbon charged sands are also of low Poisson ratio. Therefore, negative reflection coefficient at normal incidence combined with –ve gradient from top interface of soft layer shows up as increase in amplitude with offsets on CMP seismic gathers. Similarly, +ve RC at normal incidence and +ve gradient from base interface give increase in amplitude with offsets in opposite polarity. This argument is within the frame work of two term Aki and Richards approximation of Zoeppritz equation. Considering clastic regime, the increase in amplitude is inferred as class III type of AVO anomaly and is interpreted as hydrocarbon saturated porous sands. First deep water well of Mahanadi basin was drilled to probe the amplitude anomaly supported by increase in amplitudes with offsets. However, drilling results of this anomaly showed interval to be limestone encased in uncompact shale. Post drill analysis carried out to distinguish such AVO anomaly from Class III behavior of increase in amplitude with offset of hydrocarbon charged sand so that to interpret them as generated by lithology. This is discussed in this article.

Keywords: Seismic forward modeling, Reservoir Characterization, Acoustic Impedance, Poisson Ratio Amplitudes, Seismic Gathers.

Introduction

R(θ) in Zoeppritz equation (Appendix) has complicated dependence on elastic parameters of two media across the interface and angle of incidence. To relate coefficients and elastic parameters at a given incidence angle, approximated expressions as derived by Aki and Richards is instructive (Equation 1). It assumes two half space have properties i.e. the ratios $\Delta Vp/(Vp)$, $\Delta VS/(Vs)$ and $\Delta\rho/(\rho)$ much lesser than unit; It also assumes that all incidence angles are less than any critical angle and less than 90 degrees. This mathematical expression greatly simplifies the behavior of Reflection coefficients with angles and provides more insight into which changes in elastic parameters affect reflection coefficients. Fig.1 shows linearized reflection coefficients computed from equation (1) and computed from Zoeppritz equation for two models; one model yield critical angles and other yields no critical angle. Near critical angle, the linear approximation tracks exact solution computed from Zoeppritz equation quite well before it break down. For model without critical angle, the linear approximation still breaks down although at larger angles. In fact linear approximations are valid only for pre critical data, or upto 35 degree if the first critical occurs later than 35 degree.

$$R(\theta) = A + B\sin^2\theta + C\tan^2\sin^2\theta \;.......\; (1)$$

$$A = \frac{1}{2}\left[\frac{\Delta V_p}{V_p} + \frac{\Delta\rho}{\rho}\right]$$

$$B = \frac{1}{2}\frac{\Delta V_p}{V_p} - 4\left[\frac{V_s}{V_p}\right]^2\frac{\Delta V_s}{V_s} - 2\left[\frac{V_s}{V_p}\right]^2\frac{\Delta\rho}{\rho}$$

$$C = \frac{1}{2}\frac{\Delta V_p}{V_p}$$

$$R(\theta) = A + B\sin^2\theta \;.......\; (2)$$

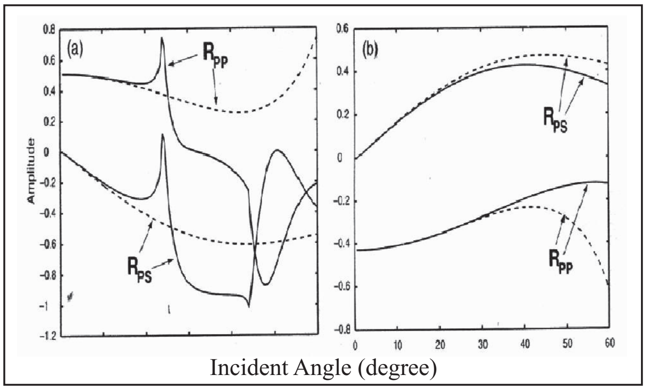

Fig. 1: Comparison of exact solution of Zoeppritz equation (solid curve) and linearized solution (dashed curve) for two half space layers models viz. $Vp2/Vp1=2.5$, $\rho2/\rho1=1.22$ and $\sigma1=\sigma2=0.25$ yields critical angles, and that of $Vp2/Vp1=0.5$, $\rho2/\rho1=0.8$ and $\sigma1=\sigma2=0.25$ does not yield any critical angle.

where ΔVp is the change in compressional velocity across the interface ($Vp2 - Vp1$), Vp is the average compressional velocity across the interface $(Vp2 + Vp1)/2$, $\Delta\rho$ is the change in density across the interface ($\rho1 - \rho2$) and ρ is the average density across the interface $(\rho1+\rho2)/2$, ΔVs is the change in shear velocity across the interface ($Vs2 - Vs1$), and VS is the average shear velocity across the interface $(Vs2+Vs1)/2$, with Vp1; Vs1; ρ1 and Vp2; Vs2; ρ2 being the medium properties in the first (overlying) and second (underlying) media, respectively.

Equation (2) Shows that R(θ) and $\sin^2\theta$ are linearly related; A and B as intercept and gradient respectively. R(θ) = A at θ=0 i.e. A is Reflection coefficient at Normal incidence. Low impedance gas sand have low Poisson ratio, therefore generates –ve RC (Reflection coefficient) and –ve gradient (-ve Poisson ratio reflectivity) from top interface and +ve reflectivity and +ve gradient (+ve Poisson ratio reflectivity) from base interface, thereby showing up on seismic gathers as increase in –ve amplitude from top and +ve amplitude from base. Contrary to this, tight sand (higher impedance) irrespective of gas or brine saturated has lesser Poisson ratio than interfacing shale, therefore it calculates +ve RC and –ve gradient from top in both the cases; showing up as +ve amplitude decreasing with offset on seismic gathers and vice versa from base interface (W. J. Ostrander, 1984). It is important to note that in this case anomalous behavior can be interpreted on A-B crossplot (Castagna, J.P. and Swan H.W., 1997, D. J. Foster, and R. G. Keys, 1999) and Smith and Gidlow's (1992) fluid factor, not on partial offset stacks and product (A and B).

Layers of relatively higher impedance and higher Poisson ratio encased in shale generate +ve RC and +ve gradient from top interface thereby showing up as increase in +ve amplitude with offsets. Similarly, negative RC and –ve gradient from base shows up as increase in –ve amplitude with offsets (W. J. Ostrander 1984).

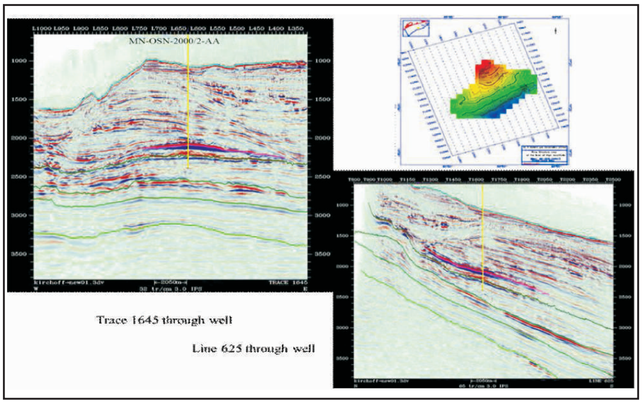

Fig.2: Targeted amplitude anomaly and its map

Case: Limestone Interfaced with Unconsolidate Shale

Amplitude anomaly seen in Mio-Pliocene interval on vertical cross sections along dip and strike profiles are mapped (Fig.2). This had been the prospective target for characterization of presence of hydrocarbon for exploration and was subjected to AVO study. An increase in amplitude with offset has been observed corresponding to the targeted events in muted gathers and on its gradient analysis (Fig. 3). Offset up to 2200m corresponding to the targeted event at well location seems to be pre-critical on gather data. AVO anomaly had been inferred as class III type of considering clastic regime, and therefore is interpreted as hydrocarbon saturated porous sand. To probe the anomaly, first offshore well in deep waters of Mahanadi basin has been drilled. However, drilling results showed interval generating increase in amplitude with offset to be carbonate encased in uncompacted shale (Fig. 4). Post drill analysis to distinguish such AVO anomaly from Class III behavior of increase in amplitude with offset so that to interpret them on seismic data to be generated by lithology.

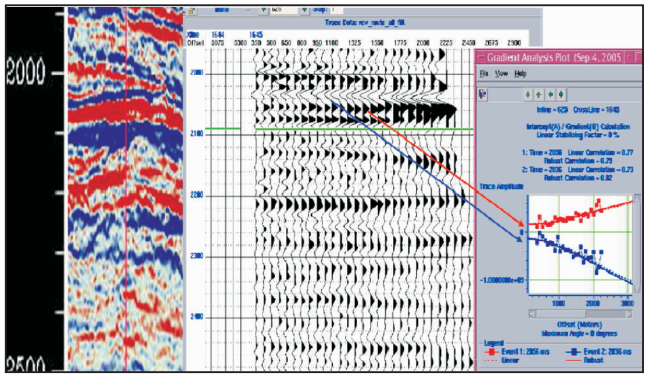

Fig.3: Increase in amplitude with offset has been observed corresponding to the targeted events.

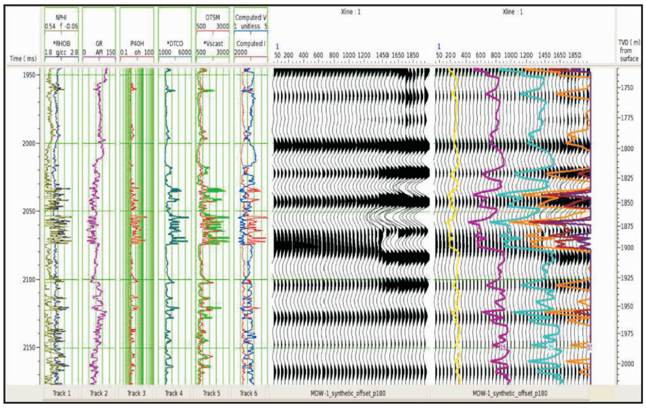

Fig. 4: Synthetic offset dependent seismic response at well location overlain by iso incident angle curves in the step of 10 degree starting from 5 degree.

Table 1: Vp, Vs and densities of shale, limestone sand and shale

	Vp	Vs	density	Vp/Vs
Shale	140	360	2.05	2.57
Limestone	90	220	2.35	2.45
Shale	140	360	2.05	

Post critical muted synthetic offset CMP gather data upto 2000m at well location shows limestone interval generating increase in amplitude with offset. Average Vp and Vs of limestone interval and that of shale just above and below is given in table1, which shows little higher Poisson ratio for limestone than shale and critical angle close to 40 degree for the top interface. Vp and Vs Crossplots show the break. in linear relationship such that the points corresponding to limestone are below the background trend of mudrock line contrary to the gas sands where points are placed above the line (Fig. 5). Vscast calculated from Vp using Castagna transform is higher than Vs contrary to the gas sands where, it is lesser than Vs. The Vs and Vscast plotted in same curve panel shows higher Vscast than Vs corresponding to limestone interval. This also translates into anomalous behavior of impedance-Poisson ratio relationship corresponding to limestone interval as members of pair move hand in hand as compared to be moving opposite as the background trend (Fig. 4). Post critical mute synthetic offset gathers are overlain by iso angle curves in the step of 10 degree starting from 5 degree to relate offsets with angles at different two way time (Fig. 4). It shows increase in amplitudes is not significantly noticeable even upto 30 degree of angle on incidence though is anomalous as compared with tight sand interval which shows decrease in amplitude with offset. Increase in amplitudes with offset is faster as approaching critical. Data has been looked into the framework of Zoeppritz equation for exact solution as assumptions made for approximated Aki-Richard equation are not met close to critical angle. ISO angle curves overlain shows, critical angle is approached even much before 2000m of offsets because of lesser depth, resulting increase in amplitude with offset as per the Zoeppritz equation (Fig. 1). The synthetic offset gathers matches well with field gathers data both at near and far offsets, explaining anomalous behavior of amplitude variation with offset given by limestone lithology (fig. 6).

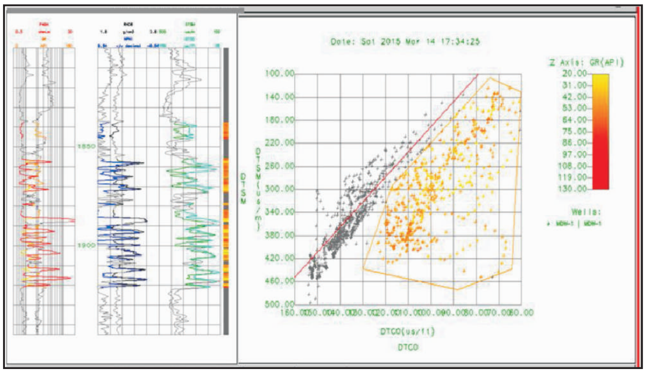

Fig.5: Cross plots show the break in linear relationship between Vp and Vs corresponds to limestone. Break is such that the points are below the background trend contrary to the gas sands where points are above, indicating higher Poisson ratio for the interval.

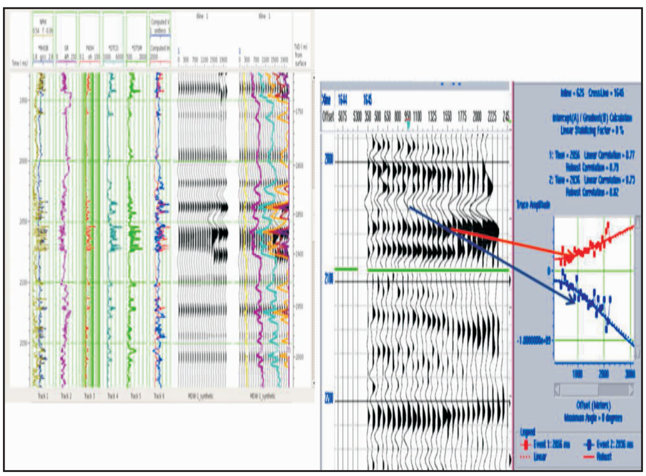

Fig.6: Synthetic gathers at well location matches with PSTM gathers; showing limestone interval generated increase in amplitude with offset.

Conclusion

Limestone in clastic regime is anomalous on seismic AVO, and therefore can be interpreted on A-B crossplots. Anomaly can be distinguished to be generated from lithology by interpreting interval as hard from study of polarity of reflected amplitudes. However, increase in amplitude with offset in this case is because of angle of incidence approaching critical.

Acknowledgement

Authors are thankful to ONGC for permitting to publish the work as the technical paper. Views expressed in the paper are those of the authors only. Authors also express their gratitude to EX-Director (Expl.), DK Pande, ONGC for giving the opportunity to work on the project and V RangaChari EX-ED-Basin Manager, KG-PG, Chennai, for guiding the project while in GEOPIC, Dehradun. Authors are thankful to RK Sharma ED-Head of Institute, IRS, ONGC and PP Deo, GM, IRS, ONGC to facilitate one of the authors to document the interpretation.

References

Castagna, J.P. and Swan H.W., 1997, Principle of AVO crossplotting: The Leading Edge v.116, no. 4, pp. 337-342.

Castagna, J.P. and Swan H.W., and Foster, D.J., 1998, Framework for AVO gradient and Intercept interpretation: Geophysics, 63, 948-956.

W. J. Ostrander Plane-wave reflection coefficients for gas sands at no normal angles of incidence GEOPHYSICS, VOL. 49, NO. IO (OCTOBER 1984); P. 1637-1648

D. J. Foster, and R. G. Keys, Interpreting AVO Responses SEG 1999, Expanded Abstracts

Appendix

Zoeppritz derived the amplitudes of the reflected and transmitted waves using the conservation of stress and displacement across the layer boundary, which gives four equations with four unknowns. Inverting the matrix form of the Zoeppritz equations gives us the exact amplitudes as a function of angle:

$$\begin{bmatrix} R_P \\ R_S \\ T_P \\ T_S \end{bmatrix} = \begin{bmatrix} -\sin\theta_1 & -\cos\phi_1 & -\sin\theta_2 & -\cos\phi_2 \\ -\cos\phi_1 & -\sin\theta_1 & -\cos\phi_2 & -\sin\theta_2 \\ -\sin 2\theta_1 & \frac{V_{p1}}{V_{s1}}\cos 2\phi_1 & \frac{\rho_2 V_{S2}^2 V_{p1}}{\rho_1 V_{S1}^2 V_{p2}}\sin 2\theta_2 & \frac{\rho_2 V_{S2} V_{p1}}{\rho_1 V_{S1}^2}\cos 2\phi_2 \\ -\cos 2\theta_1 & \frac{V_{s1}}{V_{p1}}\sin 2\phi_1 & \frac{\rho_2 V_{p2}}{\rho_1 V_{p1}}\cos 2\phi_2 & \frac{\rho_2 V_{s2}}{\rho_1 V_{p1}}\sin 2\phi_2 \end{bmatrix}^{-1} \begin{bmatrix} \sin\theta_1 \\ \cos\phi_1 \\ \sin 2\theta_1 \\ \cos 2\phi_1 \end{bmatrix}$$